The EMBO Journal vol.13 no.13 pp.3170-3181, 1994

A nuclear mutation in maize blocks the processing and translation of several chloroplast mRNAs and provides evidence for the differential translation of alternative mRNA forms

Alice Barkan, Macie Walker, Michelle Nolasco and David Johnson

Institute of Molecular Biology, University of Oregon, Eugene, OR 97403, USA

Communicated by H.Kössel

A mutant designated *crp1* (chloroplast *R*NA *p*rocessing 1) was identified in a screen for transposon-induced maize mutants with defects in chloroplast gene expression. *crp1* is a recessive, nuclear mutation that causes the loss of the cytochrome f/b_6 complex and a reduction in photosystem I. The molecular basis for these protein losses is unique relative to previously described mutants with defects in organelle gene expression; it involves defects in the metabolism of two organellar mRNAs and in the translation of two organellar proteins. Mutants lack the monocistronic forms of the *petB* and *petD* mRNAs (encoding cytochrome f/b_6 subunits), but contain normal levels of their polycistronic precursors. Pulse-labeling experiments revealed normal synthesis of the *petB* gene product, but a large decrease in synthesis of the *petD* gene product. These results suggest that *petD* sequences are more efficiently translated in a monocistronic than in a polycistronic context, thereby providing evidence that the elaborate RNA processing typical of chloroplast transcripts can play a role in controlling gene expression. Structural predictions suggest that the *petD* start codon lies in a stable hairpin in the polycistronic RNA, but remains unpaired in the monocistronic transcript. Thus, processing to a monocistronic form may increase translational efficiency by releasing the translation initiation region from inhibitory interactions with upstream RNA sequences. Synthesis of a third cytochrome f/b_6 subunit, encoded by the *petA* gene, was undetectable in *crp1*, although its mRNA appeared unaltered. Two mechanisms are consistent with the simultaneous loss of both *petA* and *petD* protein synthesis: the translation of the *petA* and *petD* mRNAs might be coupled via a mechanism independent of *crp1*, or the *crp1* gene may function to coordinate the expression of the two genes, which encode subunits of the same complex.

Key words: *Mu* transposon/organelle/photosynthetic mutant/RNA processing/translation

Introduction

In vascular plants, chloroplasts develop from undifferentiated progenitor organelles called proplastids (Kirk and Tilney-Bassett, 1978). Essential to chloroplast differentiation is the activation of chloroplast genes encoding proteins involved in photosynthesis (reviewed in Mullet, 1988). This activation is accompanied by both global and gene-specific changes in chloroplast transcription, RNA processing, RNA stability and translation (Deng and Gruissem, 1988; Barkan, 1989; Klaff and Gruissem, 1991; Baumgartner *et al.*, 1993; Gruissem and Tonkyn, 1993; Kim *et al.*, 1993; Mullet, 1993). Considering the limited coding capacity of the chloroplast genome and the fact that it contains few unidentified open reading frames, it seems likely that the bulk of the regulation is mediated by nuclear gene products. As a means towards identifying and studying nuclear gene products that regulate the expression of chloroplast genes, we are isolating transposon-induced maize mutants that fail to synthesize subsets of chloroplast-encoded proteins. An analogous approach has been fruitful in studies of chloroplast gene expression in the alga *Chlamydomonas reinhardtii*, but has not been pursued extensively in plants (Rochaix, 1992). Because fundamental differences exist between plants and algae in chloroplast gene organization and expression (Palmer, 1991), it seems likely that the mechanisms by which nuclear gene products control chloroplast gene expression may also differ significantly.

We have isolated a recessive nuclear mutation, *c*hloroplast *R*NA *p*rocessing 1 (*crp1*), from a maize line harboring active *Mu* transposons. This mutation causes the loss of the cytochrome f/b_6 complex (cyt f/b_6) and a reduction in photosystem (PS) I. Our results show that the loss of cyt f/b_6 results from defects in the processing and translation of several chloroplast mRNAs. While the precise biochemical role of the *crp1* gene product is not yet known, the mutant phenotype has been useful for addressing several fundamental questions concerning mechanisms of chloroplast gene regulation.

Most chloroplast genes in vascular plants are represented by multiple transcripts (Woodbury *et al.*, 1988; Kanno and Hirai, 1993). In some cases, these arise via processing of a single polycistronic precursor. In other cases, multiple promoters yield several overlapping transcripts (reviewed by Rochaix, 1992; Gruissem and Tonkyn, 1993; Mullet, 1993). The degree to which each RNA species contributes to the overall synthesis of the protein product is not known in any case. Substantial enzymatic machinery is required to generate these multiple transcripts, suggesting that, at least in some cases, alternate mRNA forms are functionally distinct. Experimental evidence for such functional differences has, however, been lacking. The *crp1* mutant may shed light on this issue since it lacks a subset of the processed transcripts of the maize chloroplast *psbB* gene cluster. We show here that the *petB* protein product is synthesized at the normal rate despite the absence of its monocistronic mRNA. Therefore, one or more of the polycistronic precursors must be sufficient for normal *petB* protein synthesis. In contrast, the loss of the monocistronic *petD* mRNA correlates with a substantial decrease in the rate of *petD* protein synthesis; this suggests that the missing *petD* mRNA species is the major functional template for *petD* translation *in vivo*.

Components of each multisubunit complex in the chloroplast accumulate in a stoichiometric fashion; mechanisms responsible for this are not well understood. Studies of numerous mutants have revealed that a defect in the synthesis or assembly of one subunit of a complex often leads to the destabilization of some or all of the remaining subunits (reviewed by Rochaix, 1992; Gruissem and Tonkyn, 1993). Thus, one could imagine that the rapid degradation of any subunits synthesized in excess could result in their stoichiometric accumulation in normal chloroplasts. Some evidence exists, however, for more sophisticated regulatory mechanisms, such as concerted translation of subunits that are destined to associate with one another (reviewed by Rochaix, 1992). As described above, a defect in the metabolism of the *petD* mRNA in *crp1* is correlated with the failure to synthesize *petD* protein. Although the mutation appears not to affect the structure or abundance of the *petA* mRNA, it does prevent *petA* translation. These results suggest that failure to translate the *petD* gene product may block translation of the *petA* mRNA (or vice versa). Alternatively, the *crp1* gene may act on two targets in the chloroplast genome, serving to coordinate the expression of these two independently transcribed genes. In either case, our results reveal the presence of a mechanism for coordinating the synthesis of two chloroplast-encoded proteins that will assemble into the same protein complex.

Results

crp1 is a recessive nuclear mutation that leads to the loss of cytochrome f/b_6 and PS I proteins

The *crp1* mutation arose in a maize line harboring active *Mu* transposons. Mutant seedlings were initially identified by their pale green color and seedling-lethal phenotype. The mutation is inherited through the pollen and segregates as a single, recessive mutation, indicating that it disrupts a nuclear gene. The presence of small revertant sectors (dark green stripes) on mutant leaves supports the idea that the mutation is caused by a transposon.

The pale green, seedling-lethal phenotype exhibited by *crp1* is typical of mutants lacking components of the photosynthetic electron transport chain. To detect any protein deficiencies, components of photosynthetic complexes were assayed on immunoblots (Figure 1). The cyt f/b_6 complex is severely affected by the mutation, in that its chloroplast-encoded subunits, the *petA*, *petB*, *petD* and *petG* gene products (Willey and Gray, 1988; Haley and Bogorad, 1989), accumulated to $<5\%$ of wild-type (WT) levels, and the nuclear-encoded *petC* gene product accumulated to $\sim 20\%$ of WT levels. The PS I core proteins encoded by the *psaA/B* and *psaD* genes were decreased $\sim$10-fold. Subunits of the PS II core complex (*psbB*, *psbA* and *psbD* gene products), of the thylakoid ATPase (*atpA*, *atpB* and *atpC* gene products) and of ribulose bisphosphate carboxylase (*rbcL* gene product) accumulated to normal levels. The mutation, therefore, causes the specific loss of cyt f/b_6 and PS I proteins.

The loss of monocistronic petB and petD mRNAs correlates with a loss of their protein products

The normal accumulation of ribulose bisphosphate carboxylase, ATPase and PS II indicated that a global defect in chloroplast gene expression was not responsible for the

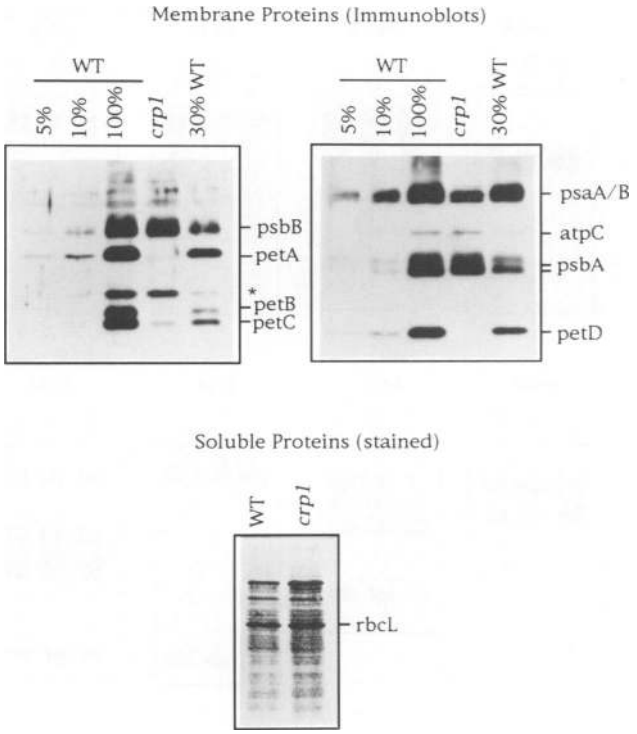

Fig. 1. Immunoblot analysis of chloroplast proteins in *crp1*. Equal amounts of WT and *crp1* leaf proteins were analyzed in adjacent lanes. Dilutions of the WT samples were included to aid in quantifying the results. Specific membrane proteins were detected by probing filters with cocktails of monospecific antisera. Total soluble proteins were detected by staining the filter with Ponceau S. Reaction of this filter with anti-Rubisco antisera confirmed the identity of the indicated *rbcL* band. The asterisk marks an unidentified protein that reacts with the *petB* antiserum. In other gels, the *petG* gene product was found to be reduced >20-fold, the *psaD* gene product was found to be reduced 10-fold, and the *psbD*, *atpA* and *atpB* gene products were detected at normal levels in *crp1* (data not shown).

crp1 phenotype. To address the possibility that the protein losses were due to defects in the metabolism of a subset of chloroplast transcripts, chloroplast mRNAs encoding missing proteins were assayed by Northern hybridization (Figure 2). RNA from a second nuclear mutant, *pet3*, that also lacks the cyt f/b_6 complex (R.Voelker and A.Barkan, submitted) is shown as well, to demonstrate that the observed changes in RNA metabolism were not the consequence of the loss of the cyt f/b_6 complex.

The chloroplast *psaA*, *psaB*, *psaC*, *psaI* and *psaJ* genes encode PS I subunits. The transcripts derived from each of these genes appeared to be unaltered in the mutant (Figure 2). Therefore, the loss of PS I is unlikely to result from a defect in the metabolism of chloroplast mRNAs encoding PS I proteins. The *petA* and *petG* transcripts (encoding cyt f/b_6 subunits) also appeared to be normal in *crp1* (Figure 2 and data not shown). However, the *petB* and *petD* transcript patterns were aberrant; the two smallest *petB* transcripts and the single smallest *petD* transcript were not detected in *crp1*.

The *petB* and *petD* genes are transcribed as part of the *psbB* gene cluster (Rock *et al.*, 1987; Tanaka *et al.*, 1987; Kohchi *et al.*, 1988; Westhoff and Hermann, 1988). Existing evidence suggests that a single promoter upstream of *psbB* is responsible for the synthesis of a tetracistronic primary transcript that is subsequently processed to yield mono-

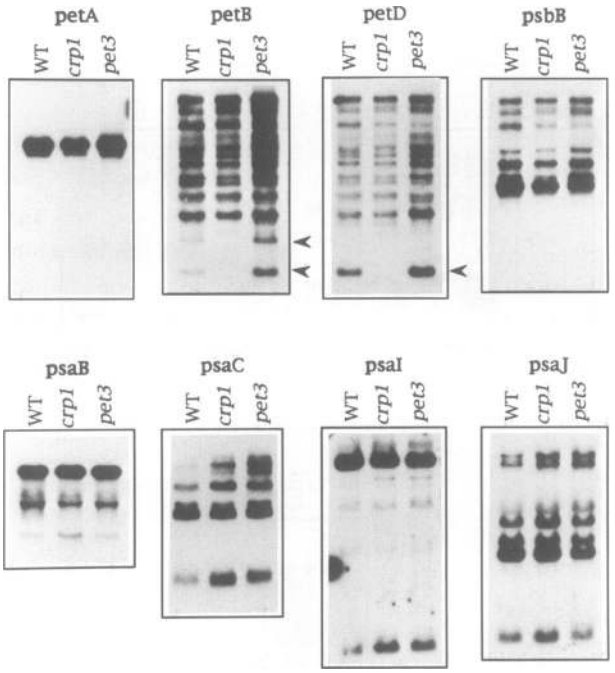

Fig. 2. Northern hybridizations of chloroplast transcripts in *crp1*. Seedling leaf RNA (2 μg) from *crp1*, a wild-type sibling (WT) or *pet3* was analyzed in each lane. Filters were probed with gene-specific probes made from cloned maize chloroplast sequences. The filters probed with *petA*, *petB*, *petD* and *psbB* were all derived from the same gel; the photographs have been aligned to facilitate comparison of transcript sizes. The filters used for detecting PS I transcripts represent several different gels. Because the *psaB* and *psaA* genes are encoded on the same mRNA, only results of probing with *psaB* are shown.

cistronic, dicistronic and tricistronic transcripts encompassing each of the four protein-coding regions (Westhoff, 1985; Tanaka *et al.*, 1987; Barkan, 1988; Kohchi *et al.*, 1988). A transcript map of this region of the maize chloroplast genome is shown in Figure 3A. Those transcripts not detected in Northern analyses of *crp1* are indicated with arrowheads. These include the monocistronic, spliced *petB* and *petD* transcripts, as well as a dicistronic *psbH–petB* transcript. Although the metabolism of the *petB* and *petD* components of the primary transcript was altered by the *crp1* mutation, there was no apparent defect in the metabolism of the upstream components (see *psbB* transcripts in Figure 2; data not shown).

The results shown in Figure 2 suggested that transcripts with ends mapping between *petB* and *petD* were absent from *crp1* chloroplasts. Since it is not possible to fully resolve all of the transcripts of the *psbB* gene cluster in agarose gels (Barkan, 1988), RNase protection was used as a more sensitive assay for transcript termini mapping in this region (Figure 3B). A non-radioactive antisense transcript spanning the *petB/petD* intergenic region (cold probe in Figure 3B) was annealed with WT or *crp1* leaf RNA. As a control, the probe was also annealed with an *in vitro* transcript designed to mimic the full-length intergenic RNA (pB/D txt in Figure 3B). Hybrids were treated with RNase T1, resolved in polyacrylamide gels and transferred to nylon membrane. Protected RNAs were detected by hybridization with short radiolabeled probes from either the *petB* or *petD* side of the intergenic region (see the diagram in Figure 3B).

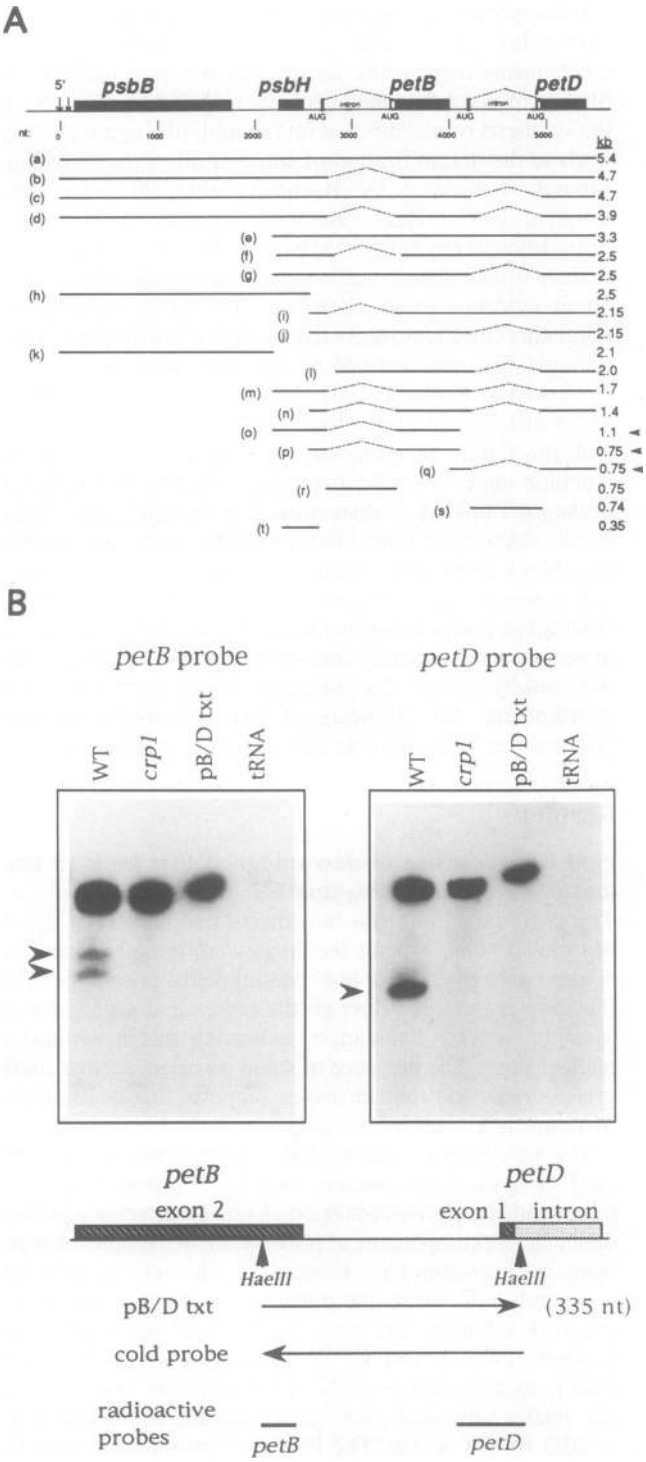

Fig. 3. Absence of transcript ends mapping between *petB* and *petD*. (**A**) Transcript map of the maize *psbB* gene cluster. The results used to generate this map were described in Barkan (1988). Arrowheads identify those transcripts not detected in *crp1*. (**B**) RNase protection analysis of transcript ends mapping between *petB* and *petD*. Leaf RNA was annealed with non-radioactive antisense transcript ('cold probe'), treated with RNase T1, fractionated in a denaturing polyacrylamide gel and transferred to nylon membrane. Protected RNA was then detected by hybridization with a short radioactive transcript ('radioactive probes') complementary to either the *petB*- or *petD*-proximal end of the cold probe. The same filter was probed first with the *petB* probe, stripped and then probed with the *petD* probe. Parallel reactions contained either tRNA or pB/D txt in place of maize RNA (tRNA and pB/D txt lanes, respectively).

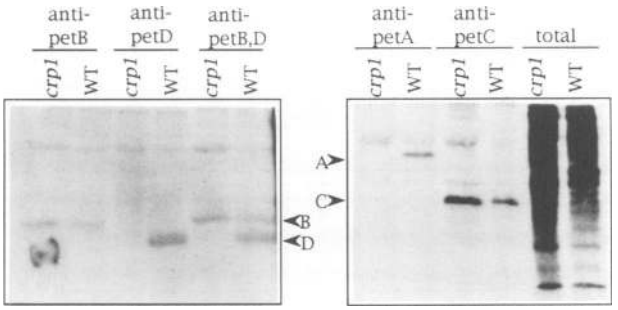

Fig. 4. *In vivo* pulse-labeling of cyt f/b_6 subunits. Leaf proteins were radiolabeled for 20 min with [^{35}S]methionine/cysteine. Total proteins were solubilized and used in immunoprecipitations with monospecific antisera. A total of 200 000 incorporated c.p.m. were used for each immunoprecipitation. Non-radioactive WT leaf protein was added to the mutant extract prior to immunoprecipitation to equalize the total amount of cyt f/b_6 proteins in the WT and *crp1* samples; the amount of WT protein used for this purpose was determined by immunoblot analysis (not shown). A, B, C and D refer to the products of the *petA*, *petB*, *petC* and *petD* genes, respectively. Lanes labeled 'total' contain 20 000 c.p.m. of each lysate.

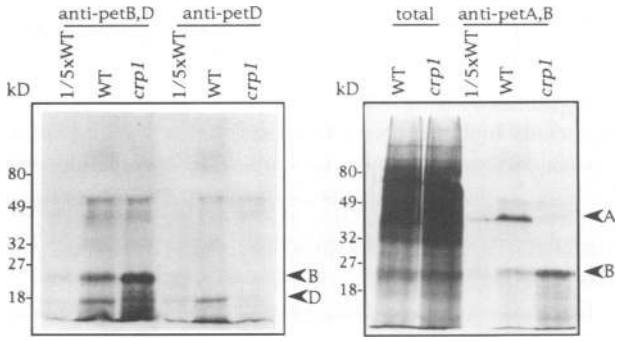

Fig. 5. *In organello* labeling of cyt f/b_6 subunits. Isolated chloroplasts were radiolabeled for 5 min with [^{35}S]methionine/cysteine. A total of 40 000 c.p.m. (incorporated) of solubilized *crp1* chloroplasts and 48 000 c.p.m. of solubilized WT chloroplasts were used for each immunoprecipitation. 5/6 of the WT sample was then loaded in the lane labeled WT and 1/6 in the lane labeled 1/5 × WT. Thus, the material present in the WT and *crp1* lanes was derived from the same amount of lysate. Lanes labeled 'total' contained 5000 c.p.m. of lysate.

Three probe fragments containing *petB* sequences were protected by WT RNA. The largest fragment corresponds to the intact intergenic RNA. The two smaller fragments correspond to transcripts with 3′ ends in this region. These results suggest that WT chloroplasts contain RNAs that end at two sites in this region (but see below). These shorter probe fragments were not detected in *crp1*, indicating the absence of homogeneous 3′ ends mapping to this region.

Two probe fragments containing *petD* sequences were protected by WT RNA. The longer fragment corresponds to the intact RNA spanning the *petB/D* intergenic region. The shorter fragment corresponds to the 5′ portion of the monocistronic *petD* mRNA. The abundance of transcript spanning the intergenic region appears to be similar in mutant and WT samples. However, shorter probe fragments were not detected in the *crp1* lane, indicating the absence of homogeneous 5′ ends mapping to this region.

Taken together, these results indicate that *crp1* chloroplasts lack transcripts with ends mapping between the *petB* and *petD* genes. The simplest mechanism to explain the concurrent and specific loss of all transcripts with ends mapping between the *petB* and *petD* coding regions is the failure of an endonuclease to cleave the primary transcript in this region. However, these losses could also result from a failure to stabilize the processed transcripts after they are formed.

The synthesis of the petA and petD gene products is decreased dramatically in crp1; the synthesis of the petB gene product is normal

To determine whether the loss of cyt f/b_6 subunits in *crp1* is due to a decrease in their rates of synthesis or a decrease in their stability, rates of protein synthesis were examined by performing pulse-labeling experiments both in intact plants and in isolated chloroplasts. Leaf proteins were pulse-labeled for 20 min by applying [^{35}S]methionine/cysteine to a transverse scratch on the leaf. Individual subunits of the cyt f/b_6 complex were then immunoprecipitated from total leaf extracts, fractionated in SDS−polyacrylamide gels and detected by autoradiography (Figure 4). We have been unable to achieve sufficient antibody excess to precipitate 100% of these antigens from WT samples. Because the mutant extracts are deficient in cyt f/b_6 proteins, a greater proportion of the radiolabeled cyt f/b_6 proteins would therefore be precipitated from mutant than from WT extracts. To compensate for this, the total amount of cyt f/b_6 protein in the two samples was equalized in the experiment shown in Figure 4 by adding non-radioactive WT proteins to the radiolabeled mutant extracts prior to immunoprecipitation.

The incorporation of radiolabel into the *petB* gene product was similar in mutant and WT (Figure 4, left panel). Although the *petB* mRNA population was altered in *crp1*, this was not reflected by a decrease in the rate of *petB* protein synthesis. In contrast, no radiolabeled *petD* gene product was detected in the mutant extracts. Co-precipitation with the *petB* and *petD* antisera revealed a dramatic difference in the ratio of labeled *petB* to *petD* in mutant and WT extracts. The synthesis of the *petC* gene product (the nuclear encoded Rieske Fe-S protein) was normal in *crp1* (Figure 4, right panel). However, no radiolabeled *petA* gene product was detected despite the normal appearance of the *petA* mRNA in Northern hybridizations (Figure 2).

It has frequently been observed that subunits of photosynthetic complexes are rapidly degraded when their assembly into a native complex is prevented (reviewed by Rochaix, 1992). The loss of the *petB* and *petC* gene products in *crp1* provides a further example of this phenomenon, since they are synthesized at the normal rate. The failure to detect radiolabeled *petD* and *petA* proteins suggested that their rates of synthesis were reduced in *crp1*. However, it was also possible that they were degraded with a half-life of several minutes. To better test their actual translation rates, a very short pulse was achieved by isolating chloroplasts and performing *in organello* translation reactions of 5 min (Figure 5). To maximize the sensitivity of the assay for the mutant extract, mutant extract was not diluted with non-radioactive WT protein prior to immunoprecipitation; this resulted in artificially high signals for cyt f/b_6 proteins in the mutant lanes. Because the rate of *petB* translation was shown to be normal in the *in vivo* labeling experiments (Figure 4), *petB* antiserum was included in several immunoprecipitations to provide an internal standard.

As expected, the *petB* signal was substantially higher in precipitations of the mutant than of the WT extract

(Figure 5). Nonetheless, no radiolabeled *petA* protein and very little radiolabeled *petD* protein was detected in the *crp1* sample. The signals were roughly quantified by comparison with dilutions of the WT samples. Taking into account the artificially high signals in the mutant lanes, the amounts of radiolabeled *petD* and *petA* proteins in the *crp1* sample were reduced by at least 10- and 20-fold, respectively. These results strongly suggest that the *crp1* mutation causes a substantial decrease in the rates of synthesis of both the *petA* and *petD* proteins.

Failure to detect labeling of a protein in pulse-labeling experiments can never prove lack of translation since protein turnover at an ever faster rate can be postulated. Therefore, additional evidence for a defect in the translation of the *petA* mRNA was obtained by analyzing the association of the *petA* mRNA with polysomes (Figure 6). Total leaf lysates were fractionated in sucrose gradients under conditions that maintained the integrity of polysomes (Barkan, 1993). The *petA* mRNA was localized in the gradients by performing Northern hybridizations with RNA purified from gradient fractions. The distribution of the chloroplast and cytosolic rRNAs was similar in the mutant and WT gradients, as revealed by staining the Northern filters with methylene blue (data not shown).

The *petA* gene in maize is represented by one predominant transcript of ~3.5 kb. This is a polycistronic mRNA, encoding *psaI* at its 5′ end and *petA* at its 3′ end (Figure 2 and A.Barkan and M.Walker, unpublished data). The *petA* mRNA was distributed in a broad peak in the sucrose gradient (Figure 6, top). The bulk of the mRNA in WT was found in the polysomal region of the gradient. However, most of this mRNA in *crp1* was associated with few or no ribosomes. Analysis of a second pair of seedlings gave similar results (not shown). The reduced sedimentation rate of the *petA* mRNA suggests a reduction in the number of associated ribosomes. Therefore, translation of one or more of the open reading frames on this mRNA is likely to be defective in a step near initiation.

PS I levels are also reduced in *crp1*. It was not possible to directly assay the synthesis of PS I subunits in pulse-labeling experiments due to lack of antisera. However, the polysomal association of chloroplast mRNAs encoding PS I proteins was tested by analyzing the distribution of the *psaA/B*, *psaC*, *psaI* and *psaJ* mRNAs in the same gradients. The dicistronic mRNA encoding *psaA* and *psaB* is distributed normally in the gradient (Figure 6, middle), suggesting that it is translated normally. The distribution of *psaJ* transcripts was also quite similar in mutant and WT, providing no evidence for a defect in *psaJ* translation (not shown). As mentioned above, *psaI* is co-transcribed with *petA*. As expected, therefore, the distribution of the predominant *psaI* transcript was identical with that of *petA* mRNA, showing a reduced association with polysomes (not shown). The low molecular weight *psaI*-specific transcript detected in leaf RNA (Figure 2) sedimented normally in the *crp1* gradient (not shown). The results did suggest, however, a possible defect in *psaC* translation: the two most prominent *psaC* transcripts in *crp1* sedimented more slowly than those in WT (Figure 6, bottom).

The structure of the petA mRNA is not detectably altered in crp1

Synthesis of the *petA* gene product could not be detected in *crp1* (Figures 4 and 5), even though the size and abundance of its mRNA appeared normal on Northern blots (Figure 2). The *petA* gene is co-transcribed with several other genes, but the polycistronic transcript is not processed to a monocistronic *petA* mRNA in maize (see Figure 2 and map in Figure 7) or rice (Kanno and Hirai, 1993). Nevertheless, since the *crp1* gene is involved in the metabolism of the *petB* and *petD* mRNAs, it seemed plausible that the failure to translate the *petA* mRNA was a consequence of a subtle change in its structure rather than a direct block in translation. To address this possibility, the positions of the 5′ and 3′ ends of the predominant *petA* transcript were compared in mutant and WT by using an RNase protection assay (Figure 7).

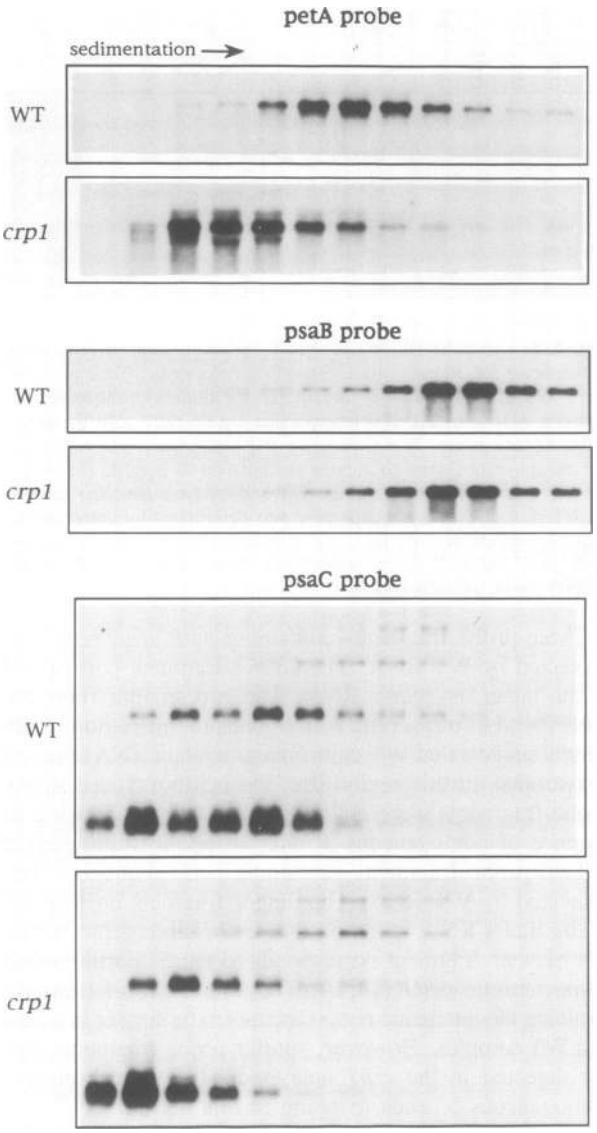

Fig. 6. Association of chloroplast mRNAs with polysomes. Total extracts of seedling leaves were fractionated on sucrose gradients. Gradients were divided into 12 fractions of equal volume. An equal proportion of the RNA purified from each fraction was analyzed by RNA gel blot hybridization. A normal sibling (WT) was analyzed in parallel with *crp1*. The rRNA distributions in these gradients and in similar gradients that contained EDTA to dissociate ribosomes suggested that the top four fractions contained particles ≤80S (i.e. monosomes and smaller). Duplicate filters were incubated with gene-specific probes containing maize chloroplast *petA*, *psaB* or *psaC* sequences. Filters were then reprobed with *psaI* and *psaJ* sequences (data not shown).

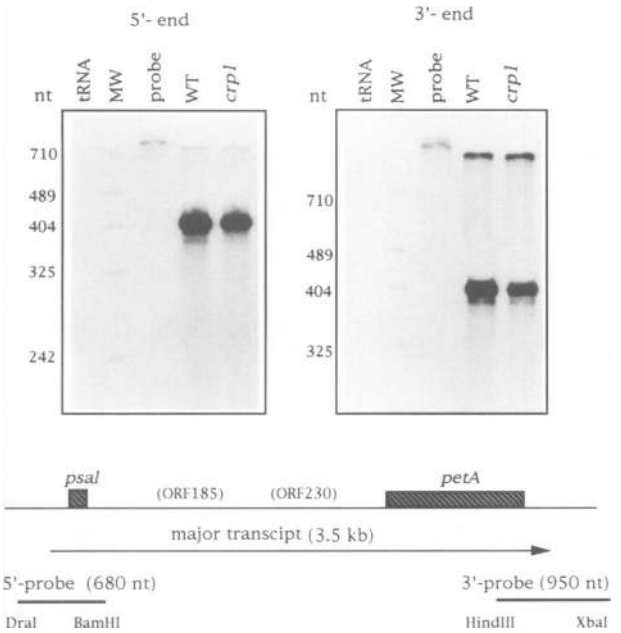

Fig. 7. RNase protection analysis of the termini of the *psaI–petA* transcript in WT and *crp1*. Radiolabeled RNA probes complementary to the predicted 5′ or 3′ ends of the transcript were annealed with 1 μg of total RNA from WT or *crp1* leaves. Hybrids were treated with RNase T1 and fractionated in a denaturing polyacrylamide gel. The probe for the 5′ end of the transcript was transcribed from a cloned *DraI–BamHI* fragment of maize chloroplast DNA, and included sequences from 370 nt upstream of the *psaI* start codon to 200 nt downstream of the *psaI* stop codon. The probe for the 3′ end of the transcript was transcribed from a cloned *HindIII–XbaI* fragment of maize chloroplast DNA, and contained sequences from 190 nt upstream to 750 nt downstream of the *petA* stop codon. Both probes included ~50 nt of vector sequence at their 5′ end. ORF185 and ORF230 are deduced open reading frames; they are found in the tobacco, rice and *Marchantia* chloroplast genomes at this position (Palmer, 1991), but have not yet been established for maize. MW, *HpaII* fragments of Bluescript SK$^+$; tRNA, parallel reactions in which tRNA was substituted for maize RNA; probe, undigested probe.

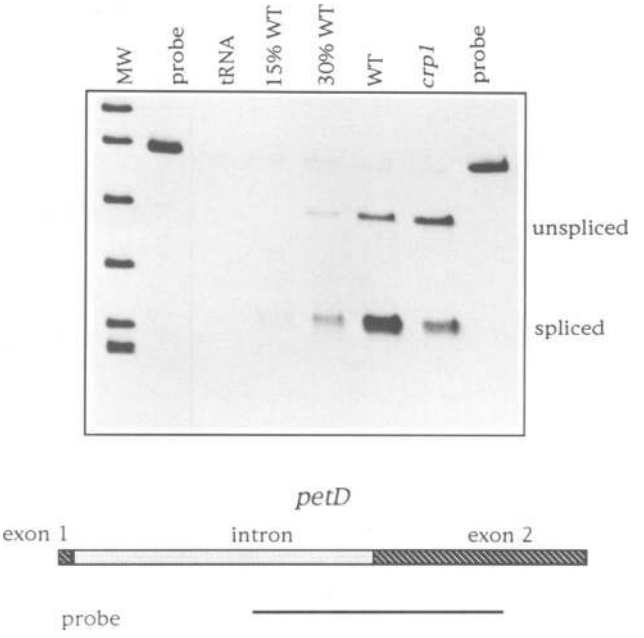

Fig. 8. S1 nuclease protection assay for spliced *petD* mRNA. Leaf RNA (0.5 μg) was annealed with a single-stranded DNA probe spanning the *petD* splice junction, and treated with S1 nuclease (Barkan, 1989). Parallel reactions contained no maize RNA (tRNA), 150 ng of WT RNA (30% WT) or 75 ng of WT RNA (15% WT). The amount of radioactivity in each band was quantified with an AMBIS scanning scintillation counter. The signals in the '30% WT' lane were 30 and 34% of that in the WT lane (spliced and unspliced, respectively), indicating that the assay was linear in this range. The band corresponding to spliced RNA contained 60% as many counts in *crp1* as in WT.

A single fragment of the probe spanning the 5′ end was protected from RNase digestion by both WT and *crp1* RNA. The approximate size of the fragment was 370 nucleotides (nt) (note that the size markers were DNA fragments, which migrate more rapidly in gels than RNA molecules of the same size). This indicates that the 5′ end of the transcript maps ~60 nt upstream from the *psaI* start codon, and is positioned similarly in mutant and WT. WT and *crp1* RNA samples also protected fragments of the 3′ probe that were indistinguishable in size. These were ~370 nt in length. The 3′ end of the *petA* mRNA, therefore, maps ~180 nt downstream from the *petA* stop codon, and is positioned similarly in mutant and WT.

Taken together with the Northern analysis of the same transcript, these results do not support a model in which the defect in *petA* translation is a consequence of a defect in the metabolism of the *petA* mRNA. Instead, these results raise two interesting possibilities: either the *petA* mRNA is not translated as a consequence of the failure to translate *petD* (i.e. their translation is coordinated) or the *crp1* gene product is required independently for the normal synthesis of both the *petA* and *petD* gene products.

The decrease in petD translation cannot be accounted for by a decrease in the total amount of spliced petD mRNA

The correlation in *crp1* between the absence of the monocistronic *petD* mRNA and the decrease in the rate of *petD* protein synthesis suggested that the monocistronic form may be the primary functional mRNA *in vivo*. Before drawing this conclusion, however, any decrease in the total amount of *petD* mRNA in the mutant must be taken into account. The *petD* open reading frame is interrupted by a single intron that is removed from only a subset of the transcripts detected on Northern blots (Rock *et al.*, 1987) (see Figure 3A). Since the monocistronic, spliced *petD* mRNA is the single most abundant spliced *petD* transcript (Barkan, 1988), its loss in *crp1* might reduce the total amount of spliced *petD* RNA available for translation.

The amount of spliced *petD* transcript was quantified by S1 nuclease protection (Figure 8). A probe spanning the *petD* 3′-splice junction was annealed to leaf RNA. Hybrids were treated with S1 nuclease and resolved in denaturing polyacrylamide gels. WT RNA protected two probe fragments, the larger one representing unspliced RNA, the smaller one representing spliced RNA. Probe fragments of the same sizes were protected by *crp1* RNA, suggesting that splicing itself is occurring faithfully in the mutant. Although the level of the spliced form was reduced somewhat in *crp1*, the <2-fold reduction was not sufficient to account for the ~10-fold reduction in the rate of *petD* protein synthesis. These results lend support to the idea that the monocistronic

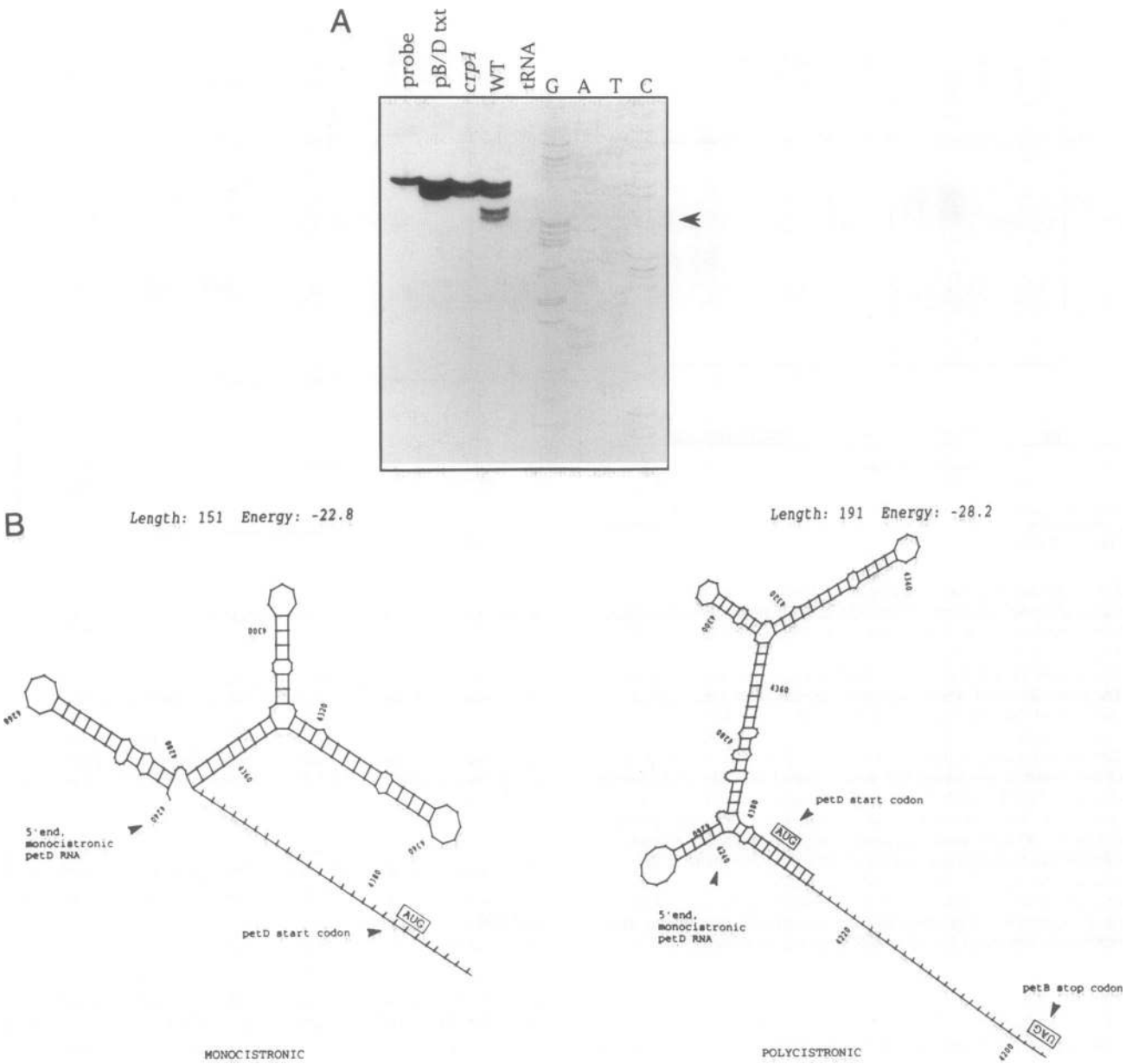

Fig. 9. Location and predicted structures of the 5′ end of the monocistronic *petD* transcript. (**A**) S1 protection mapping of the 5′ end of the monocistronic *petD* transcript. A single-stranded DNA probe was labeled at its 5′ end, located 5 nt downstream of the *petD* start codon. Probe was annealed with 1 μg WT or *crp1* leaf RNA, treated with S1 nuclease and resolved in a sequencing gel. As controls, tRNA or pB/D transcript (see Figure 3) were substituted for maize RNA. The sequencing ladder was generated from clone pB/D, containing the *petB*−*petD* intergenic region, by using the primer used in probe synthesis. (**B**) Optimal secondary structures predicted for the *petD* translation initiation region in monocistronic and polycistronic contexts. GCG FOLD (Devereux *et al.*, 1984) was used to generate the structures. The structure of uncleaved *petD* transcripts was predicted by using the entire intergenic sequence, starting at the *petB* stop codon (residue 4197) and ending 5 nt downstream of the *petD* start codon (residue 4390). The structure of the monocistronic *petD* transcript was predicted by using the nucleotide sequence between its mapped 5′ end (residue 4240) and the fifth nucleotide downstream of the *petD* start codon (residue 4390). The most stable predicted structure is shown (ΔG = −22.8 kcal). However, a structure only slightly less stable (ΔG = −20.8 kcal) is predicted if one assumes that no refolding takes place after the processing event, such that the monocistronic form folds in the same manner as residues 4240−4390 in the polycistronic form. The predicted structures of RNA molecules containing an additional 10 nt of *petD* coding sequence were not significantly different from those shown: in the polycistronic form, the *petD* translation initiation region remained unpaired and in the monocistronic form the length of the stem involving the *petD* start codon remained the same (not shown).

mRNA is a substantially better template for translation than its polycistronic precursors.

Is the petD ribosome binding site masked in the context of a polycistronic mRNA?

The RNase protection results shown in Figure 3 suggested the presence of a single 5′ end corresponding to the monocistronic *petD* mRNA. This end was mapped precisely by S1 nuclease protection using a 5′ end-labeled probe (Figure 9A). Alignment of the protected fragment with the adjacent sequencing ladder positioned this end within the sequence ATATC (see bottom of Figure 10), centered 143 nt upstream of the *petD* start codon and 37 nt downstream of the *petB* stop codon. This position was confirmed by primer extension analysis (data not shown). As expected, this end was not detected in *crp1* RNA.

The *crp1* phenotype suggested that the monocistronic *petD* mRNA is more efficiently translated than its polycistronic precursors: the absence of the monocistronic form correlated with an ~10-fold reduction in the rate of *petD* translation. To gain insight into the mechanism by which upstream RNA sequences might inhibit translation, optimal secondary structures involving the *petD* translation initiation region were predicted. The optimal structure predicted for the 5′-portion of the monocistronic *petD* mRNA contains a series of hairpins, but the sequences surrounding the start codon remain unpaired (Figure 9B). In contrast, when polycistronic precursors were mimicked by the inclusion of the entire *petB*−*petD* intergenic sequence, the *petD* start codon is predicted to lie within a stem. Examination of the nucleotide sequence immediately upstream of the 5′ end of the monocistronic *petD* transcript revealed a sequence of 13 nt with substantial complementarity to the region surrounding the *petD* start codon. The mutant phenotype and these predicted structures together support the idea that cleaving *petD* sequences from the polycistronic precursor substantially increases their translational efficiency, and that this is mediated by the removal of a segment of RNA that is complementary to the *petD* translation initiation region.

The 5′ end of the monocistronic petD mRNA and a 3′ end following petB are produced by different processing events

The origin of transcripts with ends mapping between *petB* and *petD* has not been studied. The simultaneous loss in *crp1* of transcripts with both 5′ and 3′ ends mapping in this region supports the idea that the 5′ and 3′ ends arise via a common processing event. If so, the 3′ end(s) would map upstream of the 5′ end in this region.

To evaluate this, the location of 3′ end(s) mapping in this region was determined by S1 nuclease protection with a probe labeled at its 3′ end (Figure 10). A single protected fragment was detected. Its size places the 3′ end ~30 nt downstream of the 5′ end of the monocistronic *petD* mRNA. Therefore, there is overlap between the monocistronic *petD* transcript and the transcripts represented by this 3′ end. These results are not consistent with the idea that a single endonucleolytic cleavage is responsible for generating all mRNAs with termini between *petB* and *petD*.

The RNase protection assay presented in Figure 3 provided evidence for two different 3′ ends mapping in this region. This mapping was of much lower resolution than that shown in Figure 10. Nonetheless, the results placed the ends in the same vicinity, with one end clearly downstream of the 5′ end of the monocistronic *petD* mRNA. It is not known why the S1 protection experiment revealed just one end, while the RNase protection assay revealed two. The hybrids in these experiments were quite unstable due to the A-T rich nature of the sequence. This may have led to artifactual results in one assay, but not in the other, due to differences in experimental protocol and to differences in stability between RNA−RNA and RNA−DNA duplexes.

Discussion

Genetic analysis of fungi and *C.reinhardtii* has led to the identification of nuclear genes that activate the expression of organellar genes by promoting the processing, stabilization and translation of specific organellar mRNAs (reviewed by

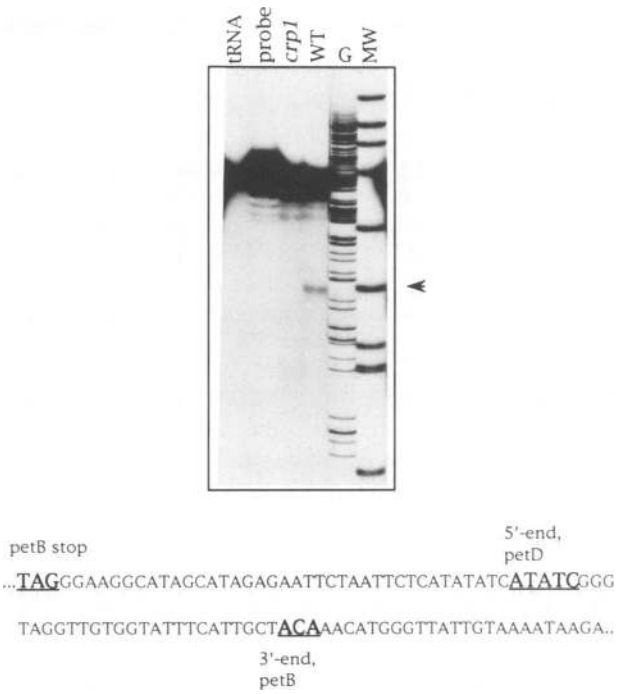

Fig. 10. Location of a 3′ end between *petB* and *petD*. A single-stranded probe radiolabeled at its 3′ end was annealed with 1 μg WT or *crp1* leaf RNA. Hybrids were treated with S1 nuclease and resolved in a sequencing gel. tRNA, parallel reaction lacking maize RNA; G, G sequencing reaction of pB/D primed with the same primer used to synthesize the probe; MW, *Hpa*II fragments of Bluescript SK+.

Costanzo and Fox, 1990; Tzagoloff and Dieckmann, 1990; Rochaix, 1992). The extent to which lessons learned from microorganisms can be extrapolated to multicellular organisms is not yet known. However, substantial differences in organelle genome organization (Palmer, 1991) and the more elaborate developmental controls on organelle function in multicellular organisms are likely to be reflected by unique mechanisms for integrating gene expression in the organelle with events in the surrounding cell. Thus, studies in plants may reveal mechanisms by which the nucleus regulates organelle function that are distinct from those in single-celled organisms. The *crp1* gene is involved in the translation of the *petA* mRNA, and in the metabolism of the *petB* and *petD* mRNAs. It therefore serves to integrate the expression of independently transcribed genes encoding subunits of a single complex. The gene is required for normal levels of PS I as well, although the mechanism for this is not yet understood. This phenotype is unique relative to mutants in *C.reinhardtii*, for which defects affecting multiple mRNAs have not been described (reviewed by Rochaix, 1992).

Although numerous non-photosynthetic mutants exist in plants (reviewed in Taylor, 1989; Rochaix, 1992), the phenotypes have rarely been studied in sufficient detail to pinpoint the molecular basis of the protein deficiencies. Chloroplast transcripts have been analyzed exhaustively in 25 maize mutants lacking either single or multiple photosynthetic complexes (Barkan *et al.*, 1986; Taylor *et al.*, 1987; Barkan, 1993; A.Barkan, unpublished data). In only three cases do defects in mRNA metabolism appear to be a component of the phenotype (*crp1*, *hcf38* and *crp2*) and in two of these the defects are global (*hcf38* and *crp2*). While nuclear mutations that block chloroplast translation globally arise rather frequently in maize (Barkan, 1993), genes that

control the translation of subsets of chloroplast mRNAs in higher plants seem to be rare. Analysis of the polysomal association of chloroplast mRNAs in three PS I and two PS II mutants failed to provide evidence for any defects in translation (A.Barkan, unpublished data). Pulse-labeling studies of three non-allelic cyt f/b_6 mutants revealed that all three are defective at a post-translational step (R.Voelker and A.Barkan, submitted). It has been proposed that the barley mutant *vir-115* is defective in the translation of the *psbA* and *psbB* mRNAs based upon the failure to detect synthesis in pulse-labeling experiments (Gamble and Mullet, 1989); however, unassembled PS II subunits can be extremely unstable (R.Voelker and A.Barkan, unpublished data) so the rather lengthy *in organello* translation reactions (20 min) might have precluded the detection of *psbA* and *psbB* translation products. Thus, while there is compelling evidence for the control of single organellar genes by single nuclear genes in fungi and *C.reinhardtii*, there is as yet no strong evidence for a similar mechanism in plants.

Our conclusion that *crp1* exhibits a loss of *petA* and *petD* translation is subject to the caveat that an extraordinarily high rate of protein turnover would also prevent the detection of protein synthesis in pulse-labeling experiments. We think this is unlikely for the following reasons. The amount of radiolabeled *petA* and *petD* protein that accumulated during a 5 min pulse was reduced at least 20- and 10-fold, respectively. Yet in studies of three non-allelic mutants lacking the cyt f/b_6 complex, synthesis of all subunits was near normal, as measured in 30 min pulse-labelings *in vivo* (R.Voelker and A.Barkan, submitted). The half-life of cyt f/b_6 subunits in the absence of assembly is shortened in such mutants, but remains on the order of 30–60 min. Finally, the failure of *petA* mRNA to associate normally with ribosomes provides independent evidence for a translation defect.

While the loss of the cyt f/b_6 complex is the most severe protein deficiency in *crp1*, the mutant also exhibits a substantial loss of the PS I core complex. The basis for this is still unknown. All chloroplast mRNAs encoding PS I proteins appear to be normal in size and abundance (Figure 2). Polysome analysis provided some suggestion that the *psaC* and/or *psaI* mRNAs might be inefficiently translated (Figure 6). However, the polycistronic nature of these transcription units makes the interpretation of such results difficult. It will, therefore, be essential to directly measure the rates of synthesis of PS I core proteins; these experiments have not yet been possible due to lack of suitable antibodies.

Role of intercistronic RNA processing in generating translatable mRNAs

Most chloroplast genes in vascular plants, but not in *C.reinhardtii*, are represented by multiple transcripts (reviewed by Rochaix, 1992; Gruissem and Tonkyn, 1993). The degree to which different transcript forms contribute to the overall synthesis of each gene product is not known. A previous experiment demonstrated that all of the many mRNAs containing intact *psbB*, *petB* and *petD* open reading frames are translated *in vivo* (Barkan, 1988), indicating that processing is not obligatory to generate functional mRNAs. However, the possibility that processing modulates translational efficiency was not eliminated. The results presented here provide strong support for the idea that the monocistronic *petD* transcript is a substantially better template for translation than its precursors, based upon two lines of evidence. First, the absence of the monocistronic transcript in the mutant correlates with a decrease of ~10-fold in the rate of *petD* translation (Figures 4 and 5). The total amount of spliced *petD* RNA sequences is reduced <2-fold (Figure 8); this is insufficient to account for the 10-fold decrease in protein synthesis. Second, precise mapping of the 5′ end of the monocistronic *petD* transcript, coupled with predictions of optimal secondary structures (Figure 9), revealed that the 13 nt immediately upstream of this 5′ end have the capacity to form a stable duplex encompassing sequences surrounding the *petD* start codon. No stable structures involving the translation initiation region were predicted for the monocistronic transcript. Taken together, these results support a model in which the monocistronic *petD* transcript is more efficiently translated than its precursors because it lacks inhibitory RNA sequences that interact with and mask the *petD* ribosome binding site. This is reminiscent of the expression of gene 1.2 in phage T7, for which alternative RNase III processing sites create mRNAs that differ in translational efficiency (Saito and Richardson, 1981).

While the removal of inhibitory sequences flanking other chloroplast coding regions may also be important for activating their translation, there is as yet no experimental evidence to support this. The absence of the monocistronic *petB* transcript had no detectable effect on *petB* protein synthesis in *crp1*, indicating that the presence on the same mRNA of downstream *petD* sequences does not inhibit *petB* translation. It remains possible, however, that *petB* must be at the 5′ end of the transcript for the most efficient translation, since the level of the abundant dicistronic *petB–petD* transcript was unaltered in the mutant (see the 1.4 kb *petB* transcript in Figures 2 and 3A).

There is strong genetic evidence for nuclear gene products that activate the translation of specific chloroplast mRNAs in *C.reinhardtii* (reviewed by Rochaix, 1992). Perhaps the complexity of transcript populations and the apparent scarcity of mRNA-specific translational activators in vascular plant chloroplasts reflects an alternative strategy for controlling translation rates: the translation of specific chloroplast mRNAs may be activated by the removal of inhibitory RNA sequences. This could be accomplished either by the action of site-specific RNases (as in the *psbB* gene cluster) or by the activation of new promoters, as proposed for the *psbD–psbC* transcription unit (Berends Sexton *et al.*, 1990; Christopher *et al.*, 1992).

Biogenesis of petB and petD transcripts

While complex transcript patterns are common in the chloroplasts of higher plants, the source of this complexity is variable. In some cases, multiple promoters are involved; in other cases, multiple RNA processing events seem to be solely responsible. Because only a single promoter has been detected in the *psbB* gene cluster (Westhoff, 1985; Tanaka *et al.*, 1987; Kohchi *et al.*, 1988), it has been assumed that RNA processing rather than multiple promoters generates the diversity of its transcripts. The phenotype of *crp1* is consistent with this assumption. The 3′ end(s) following *petB* and the 5′ end in front of *petD* are all lost as a consequence of the same mutation, suggesting that all ends mapping in the intergenic region arise via a common mechanism. Thus,

it seems unlikely that the monocistronic *petD* transcript arises from an internal promoter.

A 3′ end for transcripts containing *petB* sequences maps 30 nt downstream of the 5′ end of the monocistronic *petD* transcript. Thus, a single processing event does not give rise to both. The fact that both of these ends are absent in *crp1* suggests, nonetheless, that a common processing activity is involved in their formation. It is possible that an endonuclease recognizes a sequence or structure encompassing both of these termini, and then cleaves at either one site or the other. Alternative processing of this nature has been demonstrated in phage T7, for which a single RNase III recognition site between genes 1.2 and 1.3 can be cleaved at one of two alternative sites that lie 29 nt apart (Saito and Richardson, 1981). We cannot eliminate the possibility, however, that the *petB* 3′ ends and *petD* 5′ ends arise by different mechanisms, and that their simultaneous loss in *crp1* is the result of the loss of a shared stabilizing factor.

In addition to splicing and endonucleolytic processing, the *petB* transcript in maize is also modified by RNA editing (Freyer *et al.*, 1993). The editing event precedes both splicing and endonucleolytic cleavage since both unspliced and dicistronic transcripts are completely edited. It is possible, therefore, that failure to edit might prevent other processing events and that an editing defect in *crp1* could result in the various other properties that we observed. However, Freyer *et al.* (1993) demonstrated that the editing of the *petB* transcript is not affected by the *crp1* mutation. Therefore, a defect in *petB* editing is not responsible for the other aspects of the *crp1* phenotype.

Role of crp1 in synthesis of the cytochrome f/b_6 complex

The *crp1* mutation results in defects at several steps in the expression of genes encoding cyt f/b_6 subunits: a failure to accumulate fully processed *petB* and *petD* transcripts, failure to synthesize the *petD* gene product and failure to synthesize the *petA* gene product. Until the *crp1* gene is cloned and thoroughly analyzed, it will not be possible to conclude which of these properties are a direct consequence of the mutation and which are a secondary effect. Nonetheless, it seems very likely that *crp1* activates *petD* expression by promoting the accumulation of its fully processed transcript and not by directly activating its translation. As described above, predicted RNA structures surrounding the *petD* translation initiation region suggest that the processed transcript lacks an inhibitory structure found in its precursors.

What then is the cause of the even tighter block in *petA* translation? The structure of *petA* mRNA appears normal (Figures 2 and 7), although subtle changes in the position of its termini (± 10 nt) cannot be ruled out. Our preferred hypothesis is that *crp1* more directly activates *petA* translation, in analogy to the activation of *psbC* translation by the *C.reinhardtii* F34 and F64 genes (reviewed by Rochaix, 1992) and the activation of COXIII translation by the products of the PET122, PET494 and PET54 genes in *Saccharomyces cerevisiae* (reviewed by Costanzo and Fox, 1990). According to this scenario, *crp1* acts upon two targets in the chloroplast: it promotes the translation of the *petA* mRNA and the processing of the *petD* mRNA. A precedent for dual roles in translation and RNA metabolism exists in the PET54 gene product, which functions in yeast mitochondria to promote both the splicing of COX1 mRNA and the translation of COX3 mRNA (Valencik and McEwen, 1991).

More complex hypotheses linking the defects in *petA* and *petD* gene expression involve potential interdependencies of various translation and RNA processing events in the chloroplast. For example, the loss of *petA* translation may reflect an obligatory coupling between *petD* and *petA* protein synthesis. A coupling of this nature was suggested by Kuras and Wollman (1994) who found that deletion of the *Chlamydomonas petD* gene results in a substantial decrease in the rate of *petA* protein synthesis. While such a mechanism may contribute to the loss of *petA* translation in *crp1*, it seems unlikely to be the entire cause since the defect in *petA* translation is several-fold more severe than that in *petD* translation. It is also conceivable that the primary role of *crp1* is to activate *petA* translation, and that the processing of the *petB/petD* precursor RNA is dependent on the concurrent translation of *petA*.

The biochemical basis for the loss of all transcripts with ends mapping in the *petB–petD* intergenic region is not known, but is most simply explained by a defect in the activity of a single endonuclease that cleaves the primary transcript at two nearby sites. Over-accumulation of precursors, an expected outcome of such a defect, was not observed. However, the size heterogeneity of the precursors may make such an over-accumulation difficult to detect. It is also possible that the precursor is cleaved in the mutant, but that the cleaved forms are unstable either because the fidelity of processing is altered or because a stabilizing factor is absent that binds the 30 nt sequence shared by the processed transcripts.

Many genes in the chloroplast genome are grouped with other genes of related function into polycistronic transcription units (Woodbury *et al.*, 1988; Palmer, 1991; Rochaix, 1992; Gruissem and Tonkyn, 1993; Kanno and Hirai, 1993). This clustering may serve to coordinate the synthesis of proteins that function in common processes. However, numerous other genes with related functions are transcribed independently of one another. Regulatory mechanisms for coordinating the expression of such genes may involve global changes in rates of transcription and translation (Baumgartner *et al.*, 1989; Gamble *et al.*, 1989; Schrubar *et al.*, 1990). Superimposed upon such global changes may be the coordinate regulation of subsets of genes by mechanisms such as preferential splicing (Barkan, 1989), RNA editing (Bock *et al.*, 1993), RNA stabilization (Klaff and Gruissem, 1991; Kim *et al.*, 1993), translation (Deng and Gruissem, 1988; Liu *et al.*, 1989; Berry *et al.*, 1990) and transcription (Baumgartner *et al.*, 1993). The *crp1* gene is likely to encode a regulatory protein that links the expression of two independently transcribed genes encoding cyt f/b_6 subunits. Transposon-facilitated cloning of the *crp1* gene is in progress and will be an essential step towards defining its precise biochemical role in the chloroplast.

Materials and methods

Mutant isolation, propagation, and genetic analysis

crp1 was recovered from *Mutator* lines propagated by S.Hake, M.Freeling and co-workers (University of California, Berkeley). The mutation was originally called *hcf136*. Except where otherwise noted, plants used in these experiments were grown for 10–12 days in a growth chamber at 26°C in 16 h of light (400 $\mu E/m^2/s$) and 8 h of dark. At that time, normal and mutant seedlings had three leaves and were indistinguishable on the basis

of their size or morphology. Only fully expanded leaf tissue was used in these studies. The proportion of each leaf containing revertant tissue was very small (~1%) and should not have significantly obscured the mutant phenotype.

The *crp1* mutation was mapped to chromosome 7L by crossing heterozygous plants with a series of stocks harboring B–A translocations (Beckett, 1978). Four crosses of *crp1*/+ plants by TB-7Lb gave rise to mutant progeny with a phenotype indistinguishable from *crp1*–, i.e. a slight decrease in chlorophyll content, the loss of cytochrome f/b_6 proteins and the absence of the monocistronic *petD* mRNA. Crosses with translocation stocks involving other chromosome arms did not unmask any *crp1* mutants. Four pale green, non-photosynthetic mutations had previously been mapped to chromosome 7L; one of these (*hcf111*) was reported to lack cyt f/b_6 (Cook and Miles, 1989) and was therefore a candidate for an allele of *crp1*. Analysis of *hcf111* RNA revealed that it exhibits the same defect in *petB/D* RNA processing as *crp1* (M.Johnson, M.Bonnlander and A.Barkan, unpublished results). In complementation tests, six different crosses between *crp1*/+ and *hcf111*/+ plants each yielded one-quarter mutant progeny lacking cyt f/b_6. Therefore, *crp1* and *hcf111* do not complement and are almost certainly allelic.

Protein extraction and analysis

For immunoblot analysis, protein was extracted from seedling leaf tissue, separated into membrane and soluble fractions, and fractionated in 12% SDS–polyacrylamide gels as described previously (Barkan, 1993). Proteins were electrophoretically transferred to nitrocellulose and incubated with monospecific antisera. Antigen–antibody complexes were visualized with the Renaissance chemiluminescent detection system (New England Nuclear). While the results shown were obtained with cocktails of antibodies, individual bands were originally identified in blots probed with single antibodies.

Plants used for pulse-labeling experiments were germinated and grown in complete darkness until the third leaf was just emerging (~8 days after planting). They were then shifted into the light (400 $\mu E/m^2/s$) for 24–36 h prior to the labeling experiment. Mutant plants were identified by their decreased chlorophyll content. For *in vivo* labeling, an emory board was used to make two transverse scratches, 1 cm apart, on the upper surface of the midsection of the second leaf. The 50 μCi of [^{35}S]methionine/cysteine were brought to 10 μl with 10 mM sodium phosphate (pH 7), and 5 μl of the diluted label were applied to each scratch. Plants were incubated in an illuminated hood for 20 min, after which a 2 cm leaf segment surrounding the scratches was excised. Protein was extracted by grinding in a mortar and pestle in ice-cold protein homogenization buffer (Barkan, 1993). After removing insoluble fibers by filtration through glass wool, SDS was added to a concentration of 1% and samples were heated to 55°C for 10 min to solubilize membranes. SDS was then diluted to 0.1% by the addition of 10 vols of RIPA [0.15 M NaCl, 1% Triton X-100, 0.5% deoxycholate, 0.1% SDS, 20 mM Tris–HCl (pH 7.5), 5 μg/ml aprotinin]. For immunoprecipitations, 15 μl of each monospecific antisera were added to lysate containing 200 000 incorporated c.p.m. and incubated at 4°C overnight. Formalin-fixed Staph A cell suspension (Sigma) was washed three times in RIPA. A 10-fold excess (relative to the volume of antisera in the reaction) of 10% Staph A cell suspension was then added to the lysate–antiserum mixture and incubated for 1 h on ice. Cells were pelleted by microcentrifugation for 2 min, washed three times in RIPA and resuspended in SDS sample buffer (Laemmli, 1970). Antigens were dissociated from the cells by heating to 90°C for 5 min, cells were pelleted by microcentrifugation and the supernatant applied to SDS–polyacrylamide gels. Proteins were electrophoretically transferred to nitrocellulose. Radioactive proteins were then detected by autoradiography.

Plants used for *in organello* labeling experiments were grown under the same conditions as those used for *in vivo* labeling experiments. The apical halves of the leaves from 15 mutant or normal seedlings were pooled, added to 150 ml ice-cold GM [330 mM sorbitol, 50 mM HEPES–KOH (pH 8), 1 mM EDTA] and ground briefly in a Waring blender modified with razor blades. The material was filtered through one layer of Miracloth and the material retained was ground in fresh GM and filtered. Chloroplasts were pelleted by centrifugation at 4000 *g* for 30 s in a swinging bucket rotor and resuspended in 95 μl RM [330 mM sorbitol, 50 mM HEPES–KOH (pH 8), 10 mM $MgCl_2$]. Translation reactions were initiated by the addition of a mixture of ATP, dithiothreitol, amino acids, [^{35}S]methionine/cysteine and 2 × RM, such that the final concentrations were 1 × RM, 10 mM ATP, 10 mM dithiothreitol, 40 μM each amino acid except methionine and 50 μCi [^{35}S]methionine/cysteine. Reactions were carried out at 28°C for 5 min and stopped by the addition of an equal volume of ice-cold GM containing 10 mM methionine. Chloroplasts were pelleted by microcentrifugation for 15 s, resuspended in 50 μl GM containing 2 mM PMSF, and lysed by the addition of SDS to 1% and heating to 55°C for 10 min. No more than 1 min elapsed between the addition of cold GM/methionine and detergent lysis.

RNA and polysome extraction and analysis

Total leaf RNA and polysome fractions were prepared as described previously (Barkan, 1993). For Northern analysis, RNA samples were fractionated in denaturing formaldehyde gels, transferred to nylon membranes and hybridized with gene-specific probes as described previously (Barkan, 1993). The *psaI* probe was generated by *in vitro* transcription of a cloned 156 bp maize chloroplast DNA fragment, bounded by *Xba*I and *Bst*BI sites. This fragment includes the entire *psaI* open reading frame. The *psaJ* probe was an *in vitro* transcript of a 262 bp *Ssp*I–*Eco*RI fragment of the maize chloroplast *Bam*HI 15′ fragment, containing the entire *psaJ* coding region. The remaining probes were described in Barkan (1993).

The RNase protection experiments were performed as described by Sambrook *et al.* (1989) with minor modifications. The probes for analyzing RNAs spanning the *petB*–*petD* intergenic region were derived from plasmid pB/D (constructed by T.Tarkowski). pB/D consists of a 335 bp *Hae*III fragment of maize chloroplast DNA inserted into the *Sma*I site of Bluescript SK+. As a control in the experiments shown in Figures 3 and 9, the *in vivo* RNA spanning the *petB*–*petD* intergenic region was mimicked by pB/D txt, a transcript of the pB/D insert in the same sense as the *in vivo* RNA. The experiment shown in Figure 3 was performed by annealing 1 μg of leaf RNA or 1 ng pB/D txt with 50 ng non-radioactive antisense pB/D transcript in the presence of 10 μg of tRNA at 50°C overnight. The hybridization buffer contained 80% formamide, 400 mM NaCl, 40 mM PIPES (pH 6.4), 1 mM EDTA. Hybrids were treated with 60 U RNase T1 (BRL) at 32°C in 10 mM Tris–HCl (pH 7.5), 300 mM NaCl, 5 mM EDTA, then ethanol precipitated, denatured in formamide and fractionated in 6% polyacrylamide gels containing 7 M urea. RNA was electrophoretically transferred to nylon membrane and detected by hybridization with radioactive transcripts derived from the pB/D plasmid. Hybridization conditions were the same as those used for Northern blots. The probe to detect RNA containing *petB* sequences was obtained by T7 transcription of pB/D cleaved with *Sna*BI. This transcript includes the 93 nt between the *Hae*III site in *petB* and the *Sna*BI site 30 nt upstream of the *petB* stop codon. The probe used to detect RNA containing *petD* sequences was derived by T3 transcription of pB/D that had been cleaved with *Nsp*I. This probe includes the 144 nt between the *Hae*III site near the *petD* 5′-splice junction and the *Nsp*I site 80 nt upstream of the *petD* start codon. These probes are diagrammed in Figure 3.

The probes for mapping the *petA* mRNA termini were generated by *in vitro* transcription of cloned maize chloroplast DNA fragments. One microgram of leaf RNA was annealed with 50 000 c.p.m. of probe in the presence of 10 μg of tRNA. Hybridization, RNase digestion and denaturing gel electrophoresis were performed as described above.

The S1 mapping experiment used to assay spliced *petD* transcript was performed exactly as described in Barkan (1988). The experiment used to map the 5′ end of the monocistronic *petD* transcript was similar, except that the probe did not span the splice junction and was labeled only at its 5′ end, as follows. A 20-mer oligonucleotide complementary to the sequence immediately upstream of the *petD* 5′ splice junction was radiolabeled at its 5′ end by polynucleotide kinase in the presence of [γ-^{32}P]ATP, annealed with a single-stranded clone of the *petB*–*petD* intergenic region, and extended with Klenow polymerase in the presence of non-radioactive deoxyribonucleotides. The DNA was then cleaved in the distal polylinker with a restriction enzyme and the single-stranded probe was purified on a denaturing polyacrylamide gel. Probe and RNA were annealed overnight at 30°C in 80% formamide, 400 mM NaCl, 40 mM PIPES (pH 6.4), 1 mM EDTA. S1 nuclease reactions were performed at 30°C for 60 min. Protected fragments were resolved in denaturing polyacrylamide gels.

The probe used for the S1 mapping experiment in Figure 10 was prepared in a similar manner except that the radioactivity was incorporated only very near its 3′ end. The same primer was annealed with pB/D, extended with Klenow polymerase in the presence of non-radioactive nucleotides, and digested in the distal polylinker. The DNA was then precipitated with polyethylene glycol to remove unincorporated nucleotides and resuspended in T4 DNA polymerase buffer (Sambrook *et al.*, 1989). A small number of nucleotides from the 3′ end of the extended primer were removed by incubation for 2 min at 37°C with 3 U of T4 DNA polymerase. The 3′ end was filled in by adding dATP, dGTP, dTTP (to 0.1 mM each) and [^{32}P]dCTP (30 μCi, 3000 Ci/mmol), and incubating for 10 min at 37°C. Because two C residues are the 3′-proximal nucleotides of the chloroplast sequence in the probe, it is expected that these would be the primary radiolabeled nucleotides. However, some probe molecules may have had internal radiolabeled residues as well. The sample was denatured and the

3′ end-labeled, single-stranded probe was purified in a denaturing polyacrylamide gel.

Acknowledgements

We thank Mark Bonnlander and Melissa Mitchell for technical assistance, and Rodger Voelker and Lisa Cipolla for help with mapping and complementation crosses. Antibodies were provided by Dick Malkin (*psaD*), Sabeeha Merchant (CF1 complex) and Jean Haley (*petG*). We are grateful to Steve Rodermel for providing unpublished sequence of the maize chloroplast Bam 9 fragment, and to P.Nixon and J.Barber for providing fusion constructs of wheat *psbA* and *psbD* with which we raised antisera. We thank Sarah Hake, Michael Freeling and co-workers for providing access to their *Mutator* stocks, and Don Miles for providing mutants for complementation testing. Steve Robinson, Heather Dunstan, Rodger Voelker and Melissa Mitchell provided helpful comments on the manuscript. This work was supported by grant # DE-FG06-91ER20054 from the Department of Energy.

References

Barkan,A. (1988) *EMBO J.*, **7**, 2637–2644.
Barkan,A. (1989) *Plant Cell*, **1**, 437–445.
Barkan,A. (1993) *Plant Cell*, **5**, 389–402.
Barkan,A., Miles,D. and Taylor,W. (1986) *EMBO J.*, **5**, 1421–1427.
Baumgartner,B.J., Rapp,J.C. and Mullet,J.E. (1989) *Plant Physiol.*, **89**, 1011–1018.
Baumgartner,B.J., Rapp,J.C. and Mullet,J.E. (1993) *Plant Physiol.*, **101**, 781–791.
Beckett,J.B. (1978) *J. Hered.*, **69**, 27–36.
Berends Sexton,T., Christopher,D.A. and Mullet,J.E. (1990) *EMBO J.*, **9**, 4485–4494.
Berry,J.O., Breiding,D.E. and Klessig,D. (1990) *Plant Cell*, **2**, 795–803.
Bock,R., Hagemann,R., Kossel,H. and Kudla,J. (1993) *Mol. Gen. Genet.*, **240**, 238–244.
Christopher,D.A., Kim,M. and Mullet,J.E. (1992) *Plant Cell*, **4**, 785–798.
Cook,W.B. and Miles,C.D. (1989) *Maize Genet. Cooperation Newsl.*, **63**, 65–66.
Costanzo,M.C. and Fox,T.D. (1990) *Annu. Rev. Genet.*, **24**, 91–113.
Deng,X.-W. and Gruissem,W. (1988) *EMBO J.*, **7**, 3301–3308.
Devereux,J., Haeberli,M. and Smithies,O. (1984) *Nucleic Acids Res.*, **12**, 387–395.
Freyer,R., Hoch,B., Neckermann,K., Maier,R.M. and Kössel,H. (1993) *Plant J.*, **4**, 621–629.
Gamble,P. and Mullet,J. (1989) *J. Biol. Chem.*, **264**, 7236–7243.
Gamble,P.E., Klein,R.R. and Mullet,J.E. (1989) In Briggs,W.R. (ed.), *Photosynthesis*. Alan R.Liss, New York, pp. 285–298.
Gruissem,W. and Tonkyn,J.C. (1993) *Crit. Rev. Plant Sci.*, **12**, 19–55.
Haley,J. and Bogorad,L. (1989) *Proc. Natl Acad. Sci. USA*, **86**, 1534–1538.
Kanno,A. and Hirai,A. (1993) *Curr. Genet.*, **23**, 166–174.
Kim,M., Rapp,J.C. and Mullet,J.E. (1993) *Plant Mol. Biol.*, **22**, 447–463.
Kirk,J. and Tilney-Bassett,R. (1978) *The Plastids: Their Chemistry, Structure, Growth, and Inheritance*. Elsevier/North Holland Biomedical Press, Amsterdam.
Klaff,P. and Gruissem,W. (1991) *Plant Cell*, **3**, 517–529.
Kohchi,T., Yoshida,T., Komano,T. and Ohyama,K. (1988) *EMBO J.*, **7**, 885–891.
Kuras,R. and Wollman,F.-A. (1994) *EMBO J.*, **13**, 1019–1027.
Laemmli,U.K. (1970) *Nature*, **227**, 680.
Liu,X.-Q., Hosler,J.P., Boynton,J.E. and Gillham,N.W. (1989) *Plant Mol. Biol.*, **12**, 385–394.
Mullet,J. (1988) *Annu. Rev. Plant Physiol. Plant Mol. Biol.*, **39**, 475–502.
Mullet,J.E. (1993) *Plant Physiol.*, **103**, 309–313.
Palmer,J.D. (1991) In Bogorad,L. and Vasil,I.K. (eds), *The Molecular Biology of Plastids*. Academic Press, San Diego, CA, pp. 5–53.
Rochaix,J.-D. (1992) *Annu. Rev. Cell Biol.*, **8**, 1–28.
Rock,C.D., Barkan,A. and Taylor,W.C. (1987) *Curr. Genet.*, **12**, 69–77.
Saito,H. and Richardson,C.C. (1981) *Cell*, **27**, 533–542.
Sambrook,J., Fritsch,E.F. and Maniatis,T. (1989) *Molecular Cloning. A Laboratory Manual*. 2nd edn. Cold Spring Harbor Laboratory Press, Cold Spring Harbor, NY.
Schrubar,H., Wanner,G. and Westhoff,P. (1990) *Planta*, **183**, 101–111.
Tanaka,M., Obokata,J., Chunwongse,J., Shinozaki,K. and Sugiura,M. (1987) *Mol. Gen. Genet.*, **209**, 427–431.
Taylor,W. (1989) *Annu. Rev. Plant Physiol. Plant Mol. Biol.*, **40**, 211–233.
Taylor,W., Barkan,A. and Martienssen,R.A. (1987) *Dev. Genet.*, **8**, 305–320.
Tzagoloff,A. and Dieckmann,C.L. (1990) *Microbiol. Rev.*, **54**, 211–225.
Valencik,M.L. and McEwen,J.E. (1991) *Mol. Cell. Biol.*, **11**, 2399–2405.
Westhoff,P. (1985) *Mol. Gen. Genet.*, **201**, 115–123.
Westhoff,P. and Hermann,R.G. (1988) *Eur. J. Biochem.*, **171**, 551–564.
Willey,D.K. and Gray,J.C. (1988) *Photosynth. Res.*, **17**, 125–144.
Woodbury,N.W., Roberts,L.L., Palmer,J.D. and Thompson,W.F. (1988) *Curr. Genet.*, **14**, 75–89.

Received on March 11, 1994